Available online at www.sciencedirect.com
ScienceDirect
Polymer 48 (2007) 3013–3020
polymer
www.elsevier.com/locate/polymer

A steered molecular dynamics study on peptide sequence prediction from force-extension profiles

Linxi Zhang [a,*], Tingting Sun [b], Jun Cheng [b], Haizhu Ma [b]

[a] Department of Physics, Wenzhou University, Wenzhou 325027, PR China
[b] Department of Physics, Zhejiang University, Hangzhou 310027, PR China

Received 13 September 2006; received in revised form 1 March 2007; accepted 17 March 2007
Available online 21 March 2007

Abstract

A study of the peptide sequence prediction based on the steered molecular dynamics (SMD) method is presented. Here, 2 22-residue peptide sequences are selected. One is the neutral sequence and the other is the *LNB* sequence. Force-extension profiles are easily obtained from the steered molecular dynamics simulation. For the N_{22} sequence, it is shown that the force curve is of saw-tooth pattern. There are 22 peaks in the curves, and each peak in the curve denotes one residue in the sequence. For the *LNB* sequence, 3 force curves corresponding to the desorption from 3 different attractive surfaces are shown. The residues *L* (hydrophilic), *N* (neutral), and *B* (hydrophobic) in the sequence can be read easily from the peaks of the curves. End-to-end distance R^2 is also discussed for the 2-peptide sequences. Finally, we calculate adsorbed energy curves during the desorption process, and there are some steps in the curves, which are like the peaks in the force profiles. That is, from those steps in the energy curves, the residue prediction for the peptide sequence can also be done accurately.
© 2007 Published by Elsevier Ltd.

Keywords: Steered molecular dynamics (SMD); *LNB* sequence; Force-extension profiles

1. Introduction

Numerous functions of cells involve mechanical properties of biopolymers. A wealth of information about the mechanical properties of structural proteins has been revealed by single molecule experiments, in which proteins are stretched by mechanical forces [1–29]. Among such single molecule measurement techniques are atomic force microscopy (AFM) [30], laser optical tweezer (LOT) [31], biomembrane force probe [32], and surface force apparatus experiments [33]. Steered molecular dynamics (SMD) have also been used widely to complement these observations and provide atomic level descriptions of the underlying events [34–37]. SMD applies external forces to manipulate bio-molecules in order to probe mechanical functions, as well as accelerate processes that are otherwise too slow to model.

Unlike the SMD applications ranging from identification of ligand binding pathways [36] to the explanation of elastic properties of proteins [37], in this study we apply the SMD method to predict the peptide sequence by pulling the peptide chains from the attractive surface. As is known in biomedical research and biotechnology, the development of fast and accurate DNA sequencing methods is certain to be significant. For instance, single molecules of DNA can be detected by measuring the ionic current as a longitudinal electric field is applied to pull DNA through a pore [38–40]. However, different detection schemes such as optical [41] and capacitive [42] have also been suggested. Single nucleotide resolution has been achieved via transverse electronic transport recently [43]. An alternative DNA sequencing method is single molecule mechanical unzipping of double-stranded DNA. During the unzipping process, the binding strengths between complementary base pairs can be accurately detected by force probe. However, there are many fundamental limitations [44]. In this paper, we mainly focus on the simple sequence such as *HP*

* Corresponding author. Tel.: +86 571 88483790; fax: +86 571 87951328.
E-mail address: lxzhang@hzcnc.com (L. Zhang).

0032-3861/$ - see front matter © 2007 Published by Elsevier Ltd.
doi:10.1016/j.polymer.2007.03.046

sequence [45,46] and *LNB* sequence [47,48]. Here we predict the peptide sequence using the SMD method. In fact, the merit of SMD is that the force can be easily obtained during the pulling process.

The SMD method is used to investigate the force-extension profiles by pulling the peptide chains from the attractive surface. To consider different interactions between the residue and the attractive surface, we introduce 3 types of attractive surfaces, i.e., hydrophilic, neutral and hydrophobic. Different types of residues can be distinguished by recording the peak, which depends strongly on the attractive surface. In combination of these force curves, the total peptide sequence can be predicted. In the meantime, end-to-end distance during the desorption process is also given. Adsorbed energy changes during the desorption process for the peptide chain can also predict the different residues in the sequence. Different types of attractive surfaces, i.e., hydrophilic, neutral and hydrophobic can be achieved in the experiments.

The organization of the paper is as follows. The details of our model as well as the simulation methods are described in next section, following is the results and discussion. The last section is conclusion of our work.

2. Model and methods

2.1. The potential

A modification of the Skolnick–Honeycutt–Thirumalai model [47–49] is adopted here. The model consists of a chain of 22 residues. The residues can be of 3 types: hydrophilic (L), neutral (N) and hydrophobic (B). The residues are connected to the adjacent one by a virtual bond of length $\sigma = 3.8$ Å, which is the average distance between consecutive C_α atoms in peptides. We have studied 2 peptide models. One is $LB_9(NL)_2NBLB_3LB$, from here on referred to as *LNB* sequence, the other is a sequence of neutral residues (N_{22} sequence), which represents a simple polyamino acid that has no structural preferences.

The potential energy of a given conformation of the adsorbed peptide chains is given by

$$V = V_{\text{bond}} + V_{\text{nonbonded}} + V_{\text{bend}} + V_{\text{dih}} + V_{\text{surface}} \tag{1}$$

Here V_{bond} represents the connectivity of the chain and assumes that each bond is a stiff harmonic spring [49–51]. The harmonic potential is expressed as:

$$V_{\text{bond}} = \sum_{i=2}^{N} k_b(|\overrightarrow{u_i}| - \sigma)^2/2 \tag{2}$$

Here $\overrightarrow{u_i} = \overrightarrow{r_i} - \overrightarrow{r_{i-1}}$ is the bond vector, and we assume that the spring constant $k_b = 100$ kcal/mol Å^2 [49].

The nonbonded potential between sequence-distant residues that are not covalently bonded is represented as a sum of pairwise potentials [49,50]:

$$V_{\text{nonbonded}} = \sum_{|i-j|\geq 3} V_{ij}\left(\left|\overrightarrow{r_j} - \overrightarrow{r_i}\right|\right) \tag{3}$$

The form of potential V_{ij} depends on the types of residues i and j. The nonbonded interaction between any B–B pair is given by a Lennard–Jones potential [49,50]:

$$V_{BB} = 4\left[(\sigma/r)^{12} - (\sigma/r)^6\right] \tag{4}$$

r is the distance between the specific residue. While the interaction between L–B and L–L pairs is repulsive and long ranged:

$$V_{LB,LL} = \frac{8}{3}\left[(\sigma/r)^{12} + (\sigma/r)^6\right] \tag{5}$$

The nonbonded interaction between an N residue with any other bead takes the form:

$$V_{NB,NL,NN} = 4(\sigma/r)^{12} \tag{6}$$

The bond angle among 3 successive residues is constrained by a harmonic potential, and the bending potential is written as:

$$V_{\text{bend}} = \sum_{i=2}^{N-1} k_\theta(\theta_i - \theta_0)^2/2 \tag{7}$$

Where $\theta_0 = 105^\circ$ is the equilibrium bending angle, θ_i is the angle between vectors $\overrightarrow{u_i}$ and $\overrightarrow{u_{i+1}}$. And $k_\theta = 20$ kcal/(mol rad^2).

The dihedral angle potential, involving four successive residues, is represented by:

$$V_{\text{dih}} = \sum_{i=2}^{N-2}[A(1 + \cos\varphi_i) + B(1 + \cos 3\varphi_i)] \tag{8}$$

The dihedral angle φ_i is formed between the vectors $\overrightarrow{d_i} = \overrightarrow{u_i} \times \overrightarrow{u_{i+1}}$ and $\overrightarrow{d_{i+1}} = \overrightarrow{u_{i+1}} \times \overrightarrow{u_{i+2}}$. The parameters A and B depend on the residue type. If at most one of the residues among the four residues which define a dihedral is N, $A = B = 1.2$ kcal/mol. Otherwise $A = 0$ and $B = 0.2$ kcal/mol. However, for N_{22} sequence, $A = 0$ and $B = 1.2$ kcal/mol.

In order to simulate the desorption process for the peptide chain from the surface, we consider the attractive interactions between the residue and the surface. The form is assumed as 3–9 potential [52], and for the N_{22} sequence, it is

$$V_{\text{surface}} = \sum_{i=1}^{N} w\left[(\sigma/z_i)^9 - (\sigma/z_i)^3\right] \tag{9}$$

Here $w = 300$ kcal/mol. For the *LNB* sequence, it is

$$V_{\text{surface}} = \sum_{i=1}^{N} w_1\left[(\sigma/z_i)^9 - (\sigma/z_i)^3\right] + w_2\left[(\sigma/z_i)^9 - (\sigma/z_i)^3\right] + w_3\left[(\sigma/z_i)^9 - (\sigma/z_i)^3\right] \tag{10}$$

where, z_i is the vertical distance of residue i measured from the surface (i.e., $z = 0$), w_1 is the factor of the potential between the residue L and the attractive surface, w_2 is the factor of

the potential between the residue N and the attractive surface, and w_3 is the factor of the potential between the residue B and the attractive surface. The aim that we choose 3 types of interaction between the peptide and the surface is to distinguish different types of residues through pulling the adsorbed peptide chains away from the attractive surface. Here we use 3 groups of parameters to show different surface interactions. The first one is $w_1 = 300,\ w_2 = 100,\ w_3 = 0$ (hydrophilic), the second one is $w_1 = 0,\ w_2 = 100,\ w_3 = 300$ (hydrophobic), and the last one is $w_1 = 0,\ w_2 = 300,\ w_3 = 0$ (neutral). Here w_1, w_2, and w_3 are expressed in the unit of kcal/mol. The reason why we adopt large value w_1, w_2, and w_3 is that this paper mainly discusses the peptide sequence prediction by pulling the chain from the strongly adsorbed surface and it needs the strongly adsorbed interactions between the peptides and the surface. If the interaction between residues and the adsorbed surface is weak, the peaks in the force profiles may not be obvious. As the interaction between the peptide residues and the surface is quite larger than the interior energy of the peptide sequence, the interior structure of the sequence is not important here. For example, when the *LNB* sequence is adsorbed on the hydrophobic surface, the adsorbed energy is about 51 times larger than the interior energy of the peptide sequence.

2.2. Simulation of the dynamics

The SMD model of pulling the adsorbed peptide chains away from the attractive surface is schematically represented in Fig. 1. After the peptide sequence attains the equilibrium states on the adsorbed surface, a linear spring (force probe) is attached to one of the end residues. The stiffness of the spring is $k_0 = 945$ pN/Å. And it moves at a constant speed $v = 0.05$ Å/ps. The force probed by the spring is therefore given by Hook's law, i.e., $f = k_0(z_0 - z)$, where z and z_0 are the displacements of one of the end residues and the spring's opposite end point, respectively.

The motion of the residue is discussed by generating the atomic coordinates as a function of time. At each time step, new positions and velocities of the residues are determined by solving the equations of motion using the old positions. However, the old velocities and the accelerations are always under the restriction imposed by the law of energy conservation. In order to calculate new positions, velocities and accelerations of the residues, we use the elemental Newton equation,

$$m\frac{\mathrm{d}^2\overrightarrow{r_i}}{\mathrm{d}t^2} = \overrightarrow{F_i} = -\nabla_i V + \overrightarrow{f} \tag{11}$$

where m is the mass of a C_α atom, $\overrightarrow{r_i}$ denotes the position vector of residue i, $\overrightarrow{F_i}$ is the force on residue i due to interactions with all other residues, V is the total potential energy as discussed above, and $\overrightarrow{f}$ is a force probed by the spring. In the meantime, we choose the method originally proposed by Beeman [53].

$$\overrightarrow{r_i}(t+\Delta t) = \overrightarrow{r_i}(t) + \overrightarrow{v_i}(t)\Delta t + \frac{4\overrightarrow{F_i}(t) - \overrightarrow{F_i}(t-\Delta t)}{6m}\Delta t^2 \tag{12}$$

and

$$\overrightarrow{v_i}(t+\Delta t) = \overrightarrow{v_i}(t) + \frac{2\overrightarrow{F_i}(t+\Delta t) + 5\overrightarrow{F_i}(t) - \overrightarrow{F_i}(t-\Delta t)}{6m}\Delta t \tag{13}$$

where $\overrightarrow{v_i}$ denotes the velocity of residue i and Δt denotes the basic time step of the motion. In this work, a time step is 0.001 ps. Therefore, by pulling the chain away from the attractive surface at a constant speed, using the simulation method above, we can obtain the force-extension curves of the system. And how the chain size and energy change during the desorption process can also be discussed.

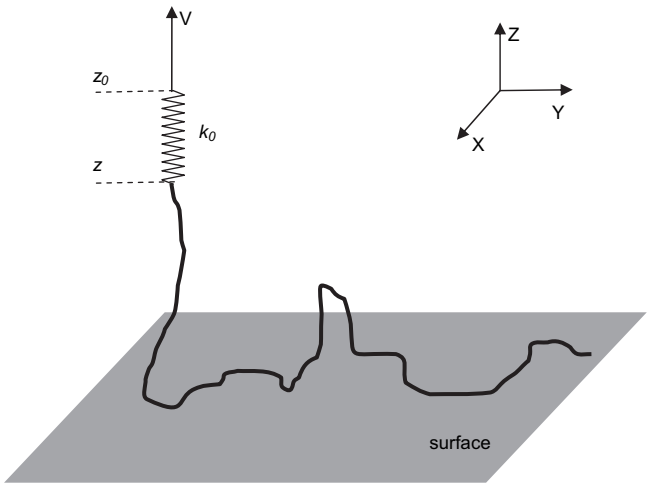

Fig. 1. A sketch of the desorption process for an adsorbed peptide chain away from the attractive surface.

3. Results and discussion

3.1. Force-extension profiles

Fig. 2 gives four representative conformations for N_{22} peptide chain during the desorption process with $z = 0$, $z = 20$ Å, $z = 60$ Å and $z = 100$ Å. Here the force is acted on one of the end residues. For $z = 0$, it means that no force is acted on the chain. Because of the interaction between the residue and the surface, the chain is adsorbed on the surface completely at this time. The second figure represents that the vertical distance between one of the end residues and the surface is 20 Å. In this conformation, a small part of peptide chain has been pulled away from the surface, and the remainder is still adsorbed on the surface. When $z = 60$ Å, opposite to $z = 20$ Å, a large part of peptide chain has been pulled away from the surface. When $z = 100$ Å, the chain has been pulled away from the surface completely, there have been no interactions between the peptide chain and the surface, and the peptide chain becomes a free chain.

Using the SMD method, we study the desorption process for the peptide chain away from the surface. This was done first by obtaining the force-extension curves for the 2 sequences, i.e., N_{22} and *LNB* sequences. Fig. 3(a) is the force profiles for the pull-off of N_{22} sequence. The inset shows

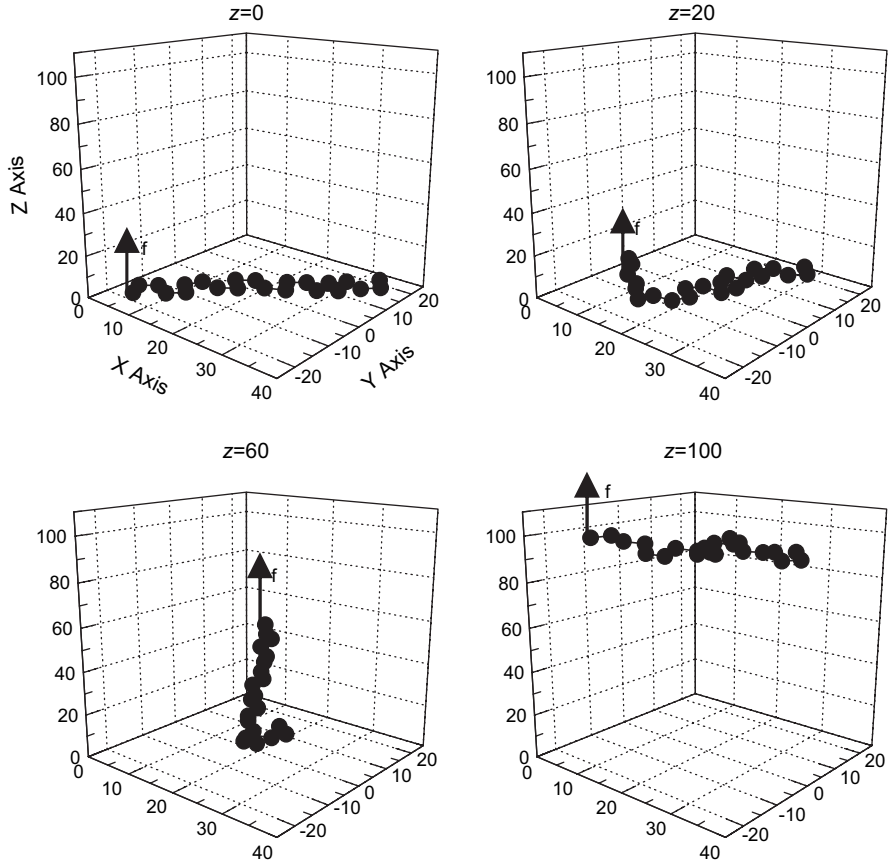

Fig. 2. Four representative conformations ($z=0$, $z=20$ Å, $z=60$ Å, $z=100$ Å) during the desorption process for the N_{22} peptide chain. The pulling rate is 0.05 Å/ps and the unit of axis is Å.

that the chain is to be pulled only one time. In order to improve the results more exactly, we have pulled the chain 50 times. The differences between these 50 pulling simulations are that the initial conformations are different. Of course, those initial conformations are all in the equilibrium states without any force acting. The large figure is the average of 50 times. When one of the end residues is pulled away from the surface with a constant rate of $v=0.05$ Å/ps, we observe that the force profile is of a saw-tooth pattern. It is important to recognize that there are 22 peaks in the force profile. The distance between 2 consecutive peaks is near to 3.8 Å, which is equal to the bond length of peptide chain. It can be explained that the saw-tooth pattern shows the residue-surface detachment. In the meantime, we can read the residue type in the sequence from the peaks of the force profiles.

For *LNB* sequence, it is assumed that if we introduce 3 types of the surfaces, i.e., hydrophilic (strong interaction with residue *L*), hydrophobic (strong interaction with residue *B*), and neutral (strong interaction with residue *N*), the force-extension profiles may be different. And from the peak position, we can read the residues *L*, *B* and *N*. According to this assumption, we introduce 3 groups of interaction factors, i.e., $w_1=300$, $w_2=100$, $w_3=0$ (hydrophilic surface), $w_1=0$, $w_2=100$, $w_3=300$ (hydrophobic surface), and $w_1=0, w_2=300, w_3=0$ (neutral surface). Fig. 3(b) shows the force-extension profile for pulling the *LNB* sequence away from the hydrophilic surface. The pulling-up trace shows 5 peaks, which means that the number of residue *L* is 5, and it is in agreement with the given *LNB* sequence. Some other findings can be deduced from the distances between the peaks. The first peak is at $z_1=3.3$ Å, it is near the first peak in Fig. 3(a). It shows that the first residue in the sequence is *L*. The situation of the second peak in the curve is located at $z_2=46.6$ Å. As $\Delta z=z_2-z_1=43.3\ \text{A}\approx 11\sigma$, this means that there are 10 residues between the first residue *L* and the second one. By using the same analyzing method, the interval between the second and third *L* residues is calculated, $\Delta z=z_3-z_2=(54.7-46.6)$ Å $=8.1$ Å $\approx 2\sigma$ (only 1 residue between the 2 adjacent residues *L*). The third residue *L* and the fourth residue *L* are apart from $\Delta z=z_4-z_3=(65.5-54.7)$ Å $=10.8$ Å $\approx 3\sigma$ (2 residues exist between the 2 adjacent residues *L*). For the interval of the last 2 peaks, it is $\Delta z=z_5-z_4=(81.3-65.5)$ Å $=15.8$ Å $\approx 4\sigma$ (3 residues is in the middle of the 2 last residues *L*). It is in good agreement with the given *LNB* sequence of $LB_9(NL)_2NBLB_3LB$ for residue *L*.

We have also studied the force profiles for pulling the chain away from the hydrophobic and neutral surfaces. The results are given in Fig. 3(c) and (d), respectively. There are 14 peaks in Fig. 3(c) and 3 peaks in Fig. 3(d). The positions of the peaks in the force profiles can be read clearly from the coordinates. By the similar method as is stated in Fig. 3(b), the orders of residue *B* and residue *N* can be deduced too. Here

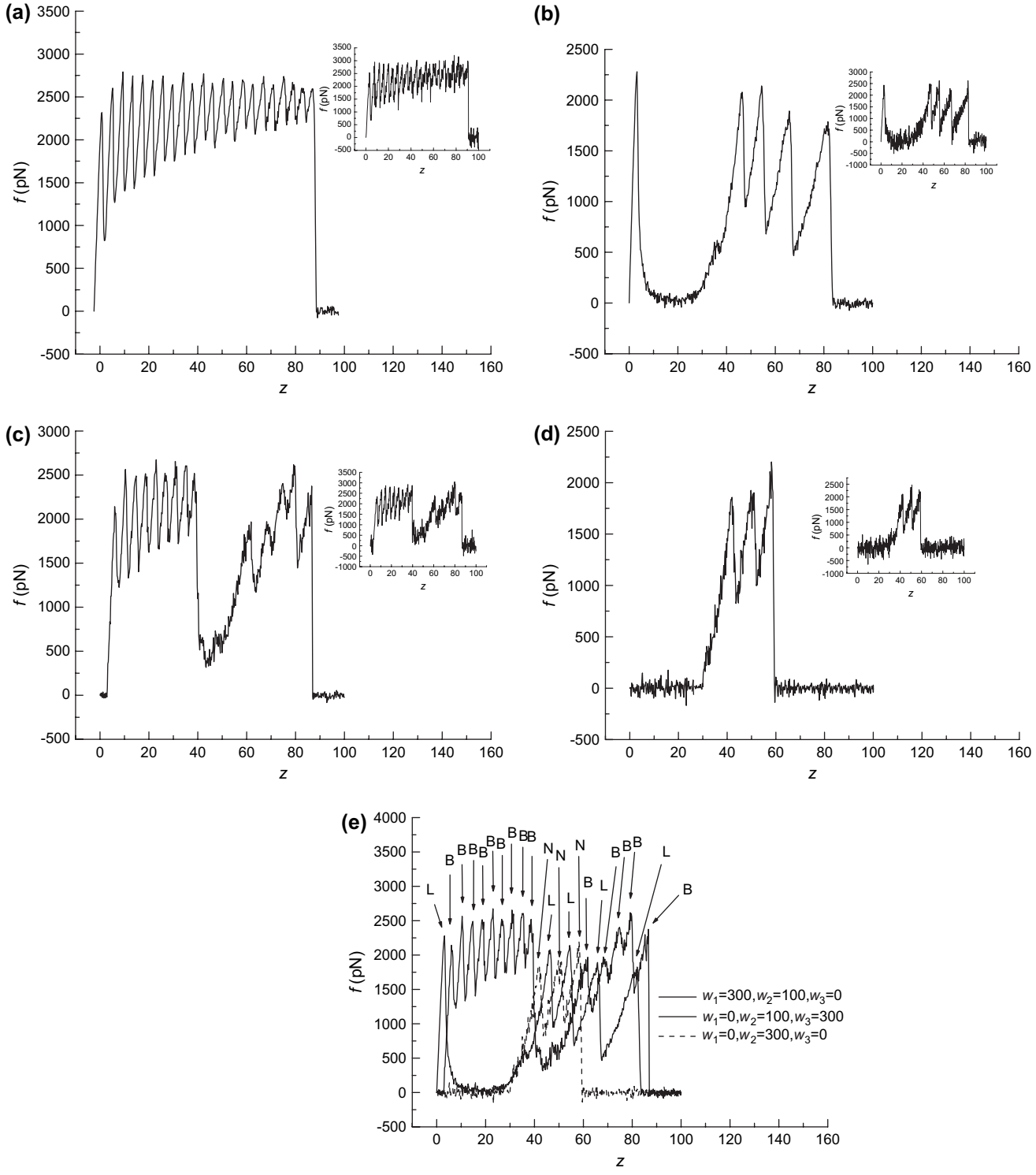

Fig. 3. Force f vs. z during the desorption process for the peptide chains. The force acts on one of the end residues. (a) N_{22} peptide chain with $w = 300$ kcal/mol; (b) *LNB* peptide chain with $w_1 = 300$ kcal/mol, $w_2 = 100$ kcal/mol, $w_3 = 0$; (c) *LNB* peptide chain with $w_1 = 0$, $w_2 = 100$ kcal/mol, $w_3 = 300$ kcal/mol; (d) *LNB* peptide chain with $w_1 = 0$, $w_2 = 300$ kcal/mol, $w_3 = 0$ (the large figure is the average of 50 times, while the small figure in the top right corner is only one time); (e) the combination of figures (b), (c) and (d). Here the pulling rate is 0.05 Å/ps, and the unit of the horizontal axis is Å.

we combine Figs. 3(b), (c) and (d) to Fig. 3(e), and draw the force curves with different lines for different attractive surfaces. The order of the residues *L*, *N* and *B* in the sequence is very obvious in Fig. 3(e). The thick solid line represents the curve for the hydrophilic surface, the common solid line shows the curve for the hydrophobic surface, and the dash line is for the neutral surface. As signed in the figure, we can read the sequence from left to right clearly, and it is $LB_9(NL)_2NBLB_3LB$, which is quite the same as given already.

Considering the actual situation of experiments, the AFM tip does not always stick to one of the end residues. Here we discuss the case that the force doesn't pull the *LNB* peptide chain at one of the end residue. In Fig. 4, we plot the force-extension curves for the cases where the force acts on the sixth residue and on the 17th residue, respectively. Here the hydrophilic surface is only considered. When the chain is pulled away from the surface, the value of the force depends on the interactions between the residues (or residue pairs) and the surface. In Fig. 4(a), since the force acts on the sixth residue, it is difficult to predict the residue from the first residue to the 11th one (i.e., $2 \times (6-1)+1=11$). However, for the later 11 residues (i.e., $22-11=11$), the position of hydrophilic in peptide sequence can be deduced by the peaks in the figure. It is shown that the second peak is located at $z = 23.4$ Å ≈ 22.8 Å $= 6\sigma$. This means that the 12th residue is *L*. Then, it is found that the interval of the third peak and the second one is $\Delta z = z_3 - z_2 = (30.7-23.4)$ Å $= 7.3$ Å $\approx 2\sigma$ (1 residue is in the middle of the 2 residues *L*). The distance of the fourth peak from the third peak is $\Delta z = z_4 - z_3 = (42.3-30.7)$ Å $= 11.6$ Å $\approx 3\sigma$ (2 residues between the 2 residues *L*). For the last 2 peaks, it is $\Delta z = z_5 - z_4 = (58.2-42.3)$Å $= 15.9$ Å $\approx 4\sigma$ (3 residues are in the last 2 residues *L*). Thus it can be seen that the position of the residue *L* in the later 11 residues can also be predicted accurately when the chain is pulled from the hydrophilic surface. Similarly, when the surface becomes hydrophobic or the neutral, the residue *B* or *N* can also be deduced by the same method.

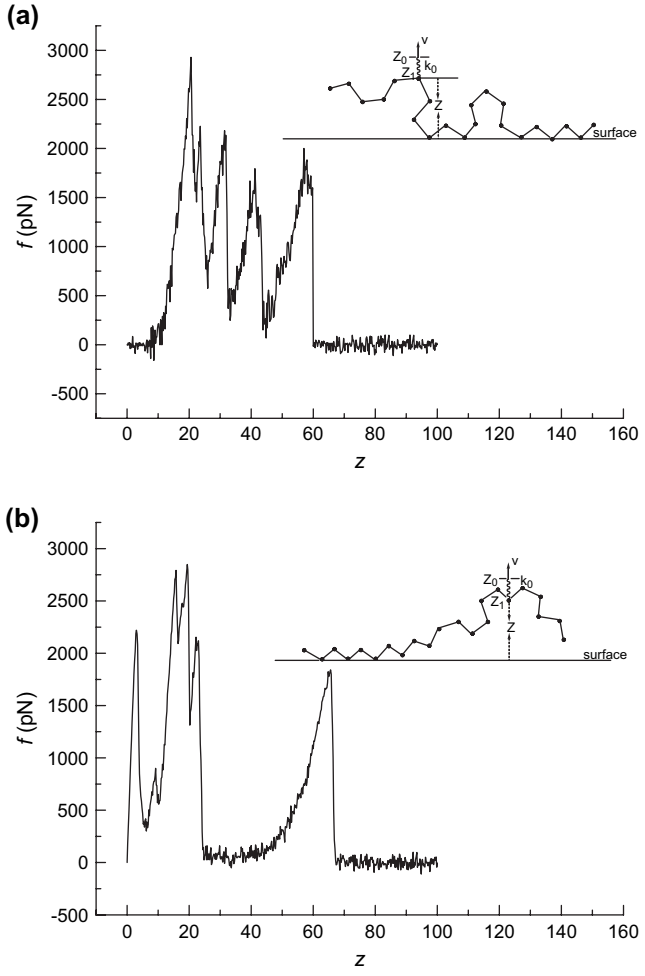

Fig. 4. Force *f* vs. *z* during the desorption process for the *LNB* peptide chains away from the attractive surface with $w_1 = 300$ kcal/mol, $w_2 = 100$ kcal/mol, $w_3 = 0$. (a) The force acts on the sixth residue; (b) the force acts on the 17th residue. The pulling rate is 0.05 Å/ps, and the unit of the horizontal axis is Å.

Since the former 11 residues are difficult to predict from Fig. 4(a), the case that the force acts on the 17th residue is also shown in Fig. 4(b). In Fig. 4(b), the later 11 residues are hard to deduce in this desorption process. However, the former 11 residues can be predicted. From Fig. 4(b), we find that there is only one peak, and the peak appears at $z > 60.8$ Å $= 16\sigma$. So it represents that there is only one residue *L* in the former 11 residues, and this residue *L* is the first residue. The position of residue *B* or *N* for the former 11 residues in the peptide chain can be predicted by the force-extension curves for the hydrophobic or neutral surfaces, respectively. Consequently, the former 11 residues can be read using the force curves when the chain is pulled at the sixth residue, as well as the later 11th residues can be predicted when chain is pulled at the 17th residue.

3.2. End-to-end distance and adsorbed energy

Fig. 5 illustrates the end-to-end distance R^2 during the desorption process from the attractive surface. Fig. 5(a) shows R^2 during the desorption process for N_{22} sequence. It is observed that the value of R^2 decreases first, then increases to a maximum. At last, it drops to the value, which is smaller than the initial value. In order to find out the difference of R^2 or 3 surfaces (hydrophilic, neutral, hydrophobic), we plot the curves of R^2 during the desorption process for *LNB* peptide chains from 3 different surfaces, Fig. 5(b). It is found that at the beginning of the desorption, the value of R^2 for the neutral surface is the smallest, and for the hydrophobic surface it is the largest one. With increasing *z*, that is, when the peptide chain is pulled away from the hydrophilic and hydrophobic surfaces, the 2 solid lines have the same trend, i.e., it first decreases, then increases, lastly drops to a little value. However, the trend of R^2 for the neutral surface is quite different. It drops earlier than the other 2 curves. The reason may be that there are only 3 residues *N* in the given *LNB* sequence, and these 3 residues *N* are in the middle of the sequence. When the surface is neutral, the interaction between the residue *N* and the surface is strong, while there is no interaction between residue *L* or *B* and the surface. This may be the reason why the end-to-end distance is smaller in the process of pulling chain from the neutral surface than the other 2 surfaces. Although a beta-hairpin can be formed for the given sequence in native state, our aim in this simulation is to predict the sequence according to the force-extension profiles; therefore, we adopt a strong attractive surface. In this case, the interior interactions between residues are smaller than the adsorption interactions, and the unique secondary structure such as alpha-helix or beta-sheet may be ignored. For example,

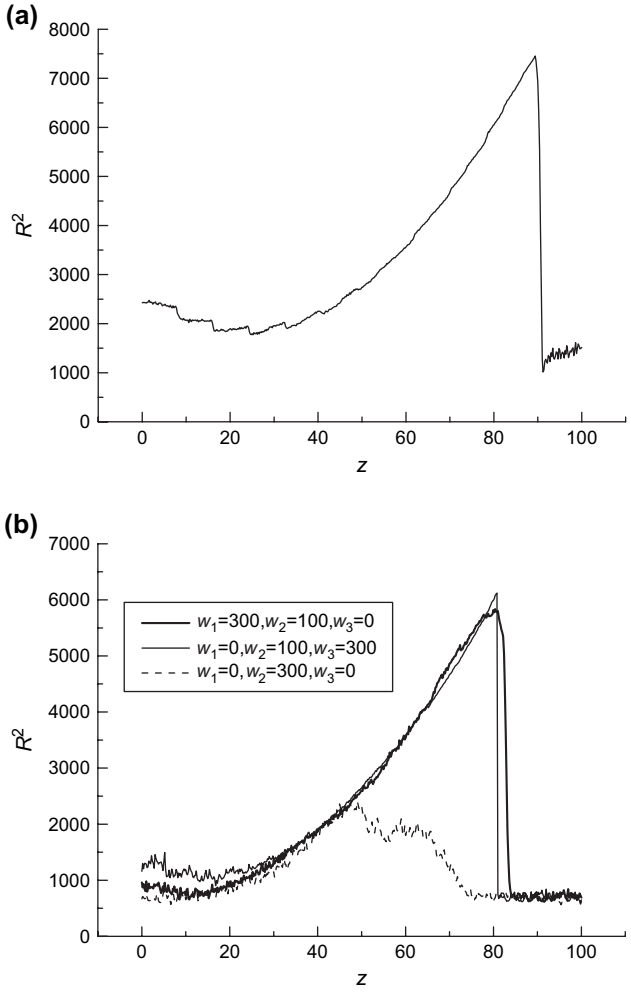

Fig. 5. End-to-end distance R^2 vs. z during the desorption process for the peptide chains. Here the force acts on one of the end residues. (a) N_{22} sequence with $w = 300$ kcal/mol; (b) *LNB* sequence with $w_1 = 300$ kcal/mol, $w_2 = 100$ kcal/mol, $w_3 = 0$; $w_1 = 0$, $w_2 = 100$ kcal/mol, $w_3 = 300$ kcal/mol; and $w_1 = 0$, $w_2 = 300$ kcal/mol, $w_3 = 0$. The pulling rate is 0.05 Å/ps. The unit of the horizontal axis is Å, and the unit of the vertical axis is Å^2.

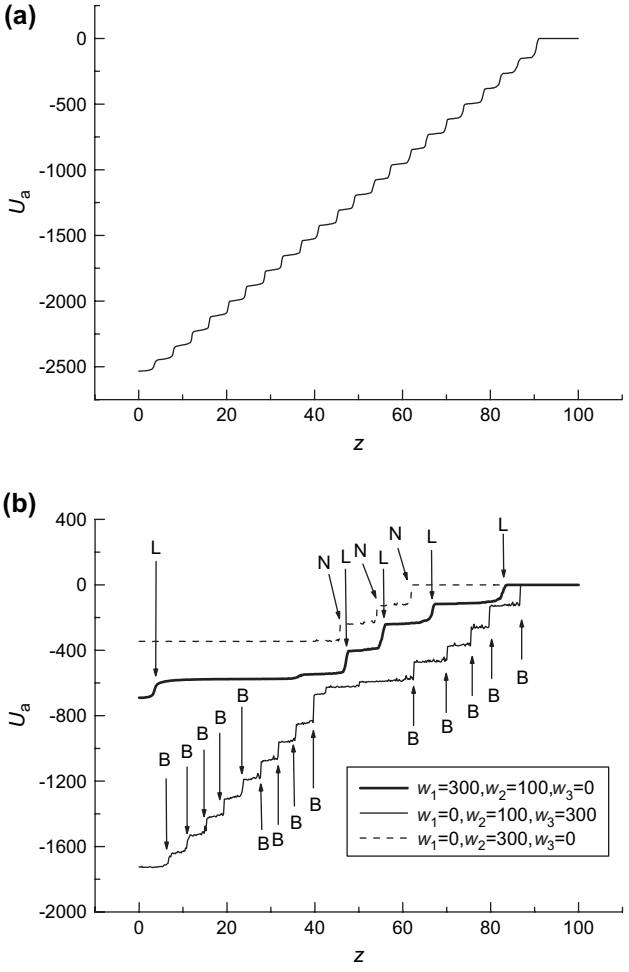

Fig. 6. Adsorbed energy U_a vs. z during the desorption process for the peptide chains. The force acts on one of the end residues. (a) N_{22} sequence with $w = 300$ kcal/mol; (b) *LNB* sequence with $w_1 = 300$ kcal/mol, $w_2 = 100$ kcal/mol, $w_3 = 0$; $w_1 = 0$, $w_2 = 100$ kcal/mol, $w_3 = 300$ kcal/mol; and $w_1 = 0$, $w_2 = 300$ kcal/mol, $w_3 = 0$. The pulling rate is 0.05 Å/ps. The unit of the horizontal axis is Å and the unit of the vertical axis is kcal/mol.

when the *LNB* sequence is adsorbed on the hydrophobic surface, the adsorbed energy is about 51 times larger than the interior energy of the peptide sequence.

In Fig. 6(a), the adsorbed energy U_a during the desorption process for the N_{22} peptide chain is plotted. The adsorbed energy U_a increases, and the curves contain 22 steps, which corresponds to the 22 peaks in the force-extension profiles. This step is reached when the residue is detached from the attractive surface, and this means that the adsorbed energy has an abrupt increase. Therefore, the steps can also be used to predict the residue sequence as the same as the peaks in force profiles. Fig. 6(b) shows the adsorbed energy during the desorption process for the *LNB* peptide chains. The thick solid line represents the curve for the hydrophilic surface, and there are 5 steps in this curve. The common solid line shows the curve for the hydrophobic surface, and there are 14 steps. The dash line is for the neutral surface, and only 3 steps are found. According to the curves of the adsorbed energy, we can also predict the residue sequence of peptide chains.

4. Conclusion

In this paper, we performed the steered molecular dynamics (SMD) method to study the pulling process of the adsorbed peptide chains away from the attractive surface. We mainly investigate the force-extension profiles for different peptide sequences such as neutral sequence (N_{22} sequence) and *LNB* sequence ($LB_9(NL)_2NBLB_3LB$). The profiles are of saw-tooth patterns. For N_{22} sequence, we find 22 peaks in the force curve. For *LNB* sequence, after considering 3 distinctive surfaces: hydrophilic, hydrophobic, and neutral, respectively, we can predict the sequence by the combination of 3 force-extension curves. On the other hand, we also discuss the end-to-end distance and the adsorbed energy during the desorption process. There are some steps in the energy curves. The steps can predict the residue in the sequence as well as

the peaks in the force curves. This work provides a feasible idea to predict the sequence of *LNB* peptide chains.

Acknowledgments

This research was financially supported by National Natural Science Foundation of China (No. 20574052), Program for New Century Excellent Talents in University (NCET-05-0538) and Natural Science Foundation of Zhejiang Province (Nos. R404047, Y405011, Y405553). The authors thank the referees for their critical reading of the manuscript and their good ideas.

References

[1] Lavery R, Lebrun A, Allemand JF, Bensimon D, Croquette V. J Phys Condens Matter 2002;14:R383–414.
[2] Becker N, Oroudjev E, Mutz S, Cleveland JP, Hansma PK, Hayashi CY, et al. Nat Mater 2003;2:278–83.
[3] Best RB, Brockwell DJ, Toca-Herrera JL, Blake AW, Smith DA, Radford SE, et al. Anal Chim Acta 2003;479:87–105.
[4] Best RB, Li B, Steward A, Daggett V, Clarke J. Biophys J 2001;81: 2344–56.
[5] Brockwell DJ, Beddard GS, Clarkson J, Zinober RC, Blake A, Trinick J, et al. Biophys J 2002;83:458–72.
[6] Erickson HP. Science 1997;276:1090–2.
[7] Fisher TE, Marsalek PE, Fernandez JM. Nat Struct Biol 2000;7:719–30.
[8] Fisher TE, Oberhauser AF, Vezquez MC, Marsalek PE, Fernandez J. Trends Biochem Sci 1999;24:379–84.
[9] Hansma HG, Pietrasanta LI. Curr Opin Chem Biol 1998;2:579–84.
[10] Hansma HG, Pietrasanta LI, Auerbach ID, Sorenson C, Golan R, Holden PA. J Biomater Sci Polymer Ed 2000;11:675–83.
[11] Kellermayer MSZ, Smith SB, Granzier HL, Bustamante C. Science 1997;276:1112–9.
[12] Li H, Carrion-Vazquez M, Oberhauser AF, Marsalek PE, Fernandez JM. Nat Struct Biol 2000;7:1117–20.
[13] Li H, Oberhauser AF, Fowler SB, Clarke J, Fernandez JM. Proc Natl Acad Sci USA 2000;97:6527–31.
[14] Marsalek PE, Lu H, Li H, Carrion-Vazquez M, Oberhauser AF, Schulten K, et al. Nature 1999;402:100–3.
[15] Oberhauser AF, Badilla-Fernandez C, Carrion-Vazquez M, Fernandez JM. J Mol Biol 2002;319:433–47.
[16] Oberhauser AF, Hansma PK, Carrion-Vazquez M, Fernandez JM. Proc Natl Acad Sci USA 2001;98:468–72.
[17] Oberhauser AF, Marszalek PE, Erickson H, Fernandez JM. Nature 1998;393:181–5.
[18] Pennisi ME. Science 1999;283:168–9.
[19] Rief M, Fernandez JM, Gaub HE. Phys Rev Lett 1998;81:4764–7.
[20] Rief M, Gautel M, Oesterhelt F, Fernandez JM, Gaub HE. Science 1997;276:1109–12.
[21] Rief M, Pascual J, Saraste M, Gaub HE. J Mol Biol 1999;286:553–61.
[22] Smith BL, Schaffer TE, Viani M, Thompson JB, Frederick NA, Kindt J, et al. Nature 1999;399:761–3.
[23] Thompson JB, Hansma HG, Hansma PK, Plaxco KW. J Mol Biol 2002;322:645–52.
[24] Thompson JB, Kindt JH, Drake B, Hansma HG, Morse DE, Hansma PK. Nature 2001;414:773–6.
[25] Tskhovrebova L, Trinic JA, Sleep JA, Simmons RM. Nature 1997;387: 308–12.
[26] Viani MB, Schaffer TE, Paloczi GT, Pietrasanta LI, Smith BL, Thompson JB, et al. Rev Sci Instrum 1999;70:4300–3.
[27] Viani MB, Schaffer TE, Chand A, Rief M, Gaub HE, Hansma PK. J Appl Phys 1999;86:2258–62.
[28] Zhuang X, Rief M. Curr Opin Struct Biol 2003;13:88–97.
[29] Zinober RC, Brockwell DJ, Beddard GS, Blake AW, Olmsted PD, Radford SE, et al. Protein Sci 2002;11:2759–65.
[30] Binning G, Quate CF, Gerber G. Phys Rev Lett 1986;56:930–3.
[31] Ashkin A, Dziedzic JM. Science 1987;235:1517–20.
[32] Evans E, Ritchie K, Merkel R. Biophys J 1995;68:2580–7.
[33] Israelachvili JN. Intermolecular and surface forces. London: Academic Press; 1992.
[34] Isralewitz B, Baudry J, Gullingsrud J, Kosztin D, Schulten K. J Mol Graph Model 2001;19:13–25.
[35] Isralewitz B, Gao M, Schulten K. Curr Opin Struct Biol 2001;11: 224–30.
[36] Izrailev S, Stepaniants S, Balsera M, Oono Y, Sechulten K. Biophys J 1997;72:1568–81.
[37] Lu H, Schulten K. Proteins Struct Func Genetics 1999;35:453–63.
[38] Meller A, Nivon L, Branton D. Phys Rev Lett 2001;86:3435–9.
[39] Chen P, Gu J, Brandin E, Kim YR, Wang Q, Branton D. Nano Lett 2004;4:2293–8.
[40] Fologea D, Gershow M, Ledden B, McNabb DS, Golovchenko JA, Li J. Nano Lett 2005;5:1905–9.
[41] Braslavsky I, Hebert B, Kartalov E, Quake SR. Proc Natl Acad Sci USA 2003;100:3960–4.
[42] Gracheva ME, Xiong A, Aksimentiev A, Schulten K, Timp G, Leburton JP. Nanotechnology 2006;17:622–33.
[43] Lagerqvist J, Zwolak M, Di Ventra M. Nano Lett 2006;6:779–82.
[44] Voulgarakis NK, Redondo A, Bishop AR, Rasmussen Kø. Nano Lett 2006;6:1483–6.
[45] Dill KA. Biochemistry 1985;24:1501–9.
[46] Lau KF, Dill KA. Macromolecules 1989;22:3986–97.
[47] Kolinsky A, Skolnick J, Yaris R. Biopolymers 1987;26:937–62.
[48] Honeycutt JD, Thirumalai D. Proc Natl Acad Sci USA 1990;87:3526–9.
[49] Kirmizialtin S, Ganesan V, Makarov DE. J Chem Phys 2004;121: 10268–77.
[50] Guo Z, Thirumalai D. J Chem Phys 1992;97:525–35.
[51] Veitshans T, Klimov D, Thirumalai D. Fold Des 1996;2:1–22.
[52] Li FY, Yuan JM, Mou CY. Phys Rev E 2001;63:021905–10.
[53] Beeman D. J Comp Phys 1976;20:130–9.